



Since January 2020 Elsevier has created a COVID-19 resource centre with free information in English and Mandarin on the novel coronavirus COVID-19. The COVID-19 resource centre is hosted on Elsevier Connect, the company's public news and information website.

Elsevier hereby grants permission to make all its COVID-19-related research that is available on the COVID-19 resource centre - including this research content - immediately available in PubMed Central and other publicly funded repositories, such as the WHO COVID database with rights for unrestricted research re-use and analyses in any form or by any means with acknowledgement of the original source. These permissions are granted for free by Elsevier for as long as the COVID-19 resource centre remains active.



Cardiothoracic Imaging



Quantitative assessment of lung involvement on chest CT at admission: Impact on hypoxia and outcome in COVID-19 patients

Antonio Esposito^{a,b,*,1}, Anna Palmisano^{a,b,1}, Roberta Cao^{a,b}, Paola Rancoita^c, Giovanni Landoni^{b,d}, Daniele Grippaldi^{a,b}, Edda Boccia^e, Michele Cosenza^{a,b}, Antonio Messina^{a,b}, Salvatore La Marca^{a,b}, Diego Palumbo^{a,b}, Clelia Di Serio^{b,c}, Marzia Spessot^f, Moreno Tresoldi^g, Paolo Scarpellini^h, Fabio Ciceri^{b,i}, Alberto Zangrillo^{b,d}, Francesco De Cobelli^{a,b}

^a Experimental Imaging Center, Radiology Unit, IRCCS San Raffaele Hospital, Milan, Italy

^b School of Medicine, Vita-Salute San Raffaele University, Milan, Italy

^c University Centre for Statistics in the Biomedical Sciences, Vita-Salute San Raffaele University, Milan, Italy

^d Department of Anesthesia and Intensive Care, IRCCS San Raffaele Scientific Institute, Milan, Italy

^e Imaging analysis and post-processing, Experimental Imaging Center, IRCCS San Raffaele Hospital, Milan, Italy

^f Emergency Medicine, Emergency Department, IRCCS San Raffaele Hospital, Milan, Italy

^g Unit of General Medicine and Advanced Care, IRCCS San Raffaele Scientific Institute, Milan, Italy

^h Infectious Diseases Department, IRCCS San Raffaele Scientific Institute, Milan, Italy

ⁱ Hematology and Bone Marrow Transplantation, IRCCS San Raffaele Scientific Institute, Italy

ARTICLE INFO

Keywords:

Covid-19

Quantitative CT

Artificial intelligence

Pneumonia

Outcome

ABSTRACT

Background: The aim of this study was to quantify COVID-19 pneumonia features using CT performed at time of admission to emergency department in order to predict patients' hypoxia during the hospitalization and outcome.

Methods: Consecutive chest CT performed in the emergency department between March 1st and April 7th 2020 for COVID-19 pneumonia were analyzed. The three features of pneumonia (GGO, semi-consolidation and consolidation) and the percentage of well-aerated lung were quantified using a HU threshold based software. ROC curves identified the optimal cut-off values of CT parameters to predict hypoxia worsening and hospital discharge. Multiple Cox proportional hazards regression was used to analyze the capability of CT quantitative features, demographic and clinical variables to predict the time to hospital discharge.

Results: Seventy-seven patients (median age 56-years-old, 51 men) with COVID-19 pneumonia at CT were enrolled. The quantitative features of COVID-19 pneumonia were not associated to age, sex and time-from-symptoms onset, whereas higher number of comorbidities was correlated to lower well-aerated parenchyma ratio ($\rho = -0.234$, $p = 0.04$) and increased semi-consolidation ratio ($\rho = -0.303$, $p = 0.008$).

Well-aerated lung ($\leq 57\%$), semi-consolidation ($\geq 17\%$) and consolidation ($\geq 9\%$) predicted worst hypoxemia during hospitalization, with moderate areas under curves (AUC 0.76, 0.75, 0.77, respectively). Multiple Cox regression identified younger age ($p < 0.01$), female sex ($p < 0.001$), longer time-from-symptoms onset ($p = 0.049$), semi-consolidation $\leq 17\%$ ($p < 0.01$) and consolidation $\leq 13\%$ ($p = 0.03$) as independent predictors of shorter time to hospital discharge.

Conclusion: Quantification of pneumonia features on admitting chest CT predicted hypoxia worsening during hospitalization and time to hospital discharge in COVID-19 patients.

Abbreviations: AUC, area under curve; ED, emergency department; COVID-19, coronavirus disease 2019; GGO, ground glass opacity; HU, Hounsfield Unit; ROC, receiver operating characteristics curve.

* Corresponding author at: IRCCS San Raffaele Scientific Institute and Vita-Salute San Raffaele University, Via Olgettina 60, 20132 Milan, Italy.

E-mail address: esposito.antonio@hsr.it (A. Esposito).

¹ Antonio Esposito and Anna Palmisano equally contributed to the study.

<https://doi.org/10.1016/j.clinimag.2021.04.033>

Received 16 June 2020; Received in revised form 14 April 2021; Accepted 18 April 2021

Available online 29 April 2021

0899-7071/© 2021 Elsevier Inc. All rights reserved.

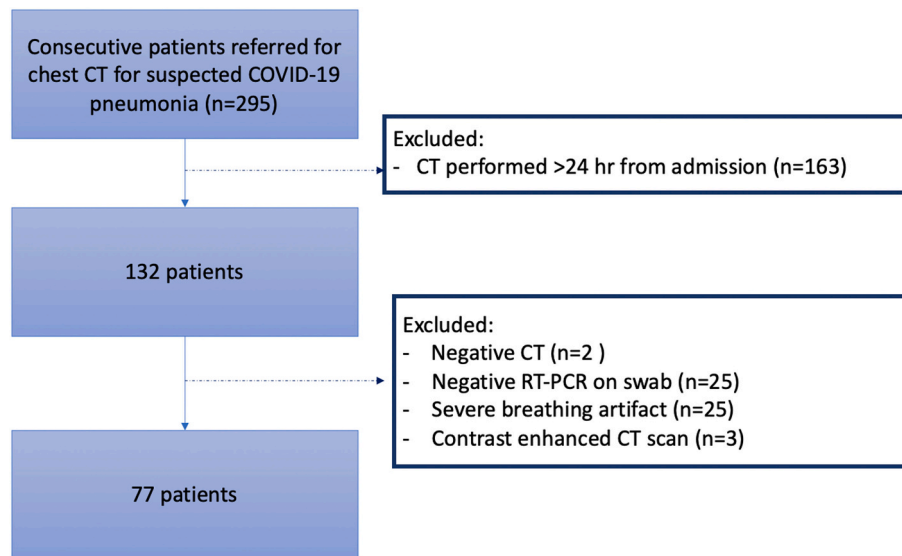


Fig. 1. Flowchart of patient selection. Abbreviations: CT = computed tomography; RT-PCR = real time polymerase chain reaction.

1. Introduction

SARS-CoV-2 infection causes a systemic disease, namely coronavirus disease 2019 (COVID-19), dominated by lung involvement. Most of patients develop mild to moderate symptoms, but few of them rapidly progress toward severe pneumonia, pulmonary edema, and acute respiratory distress syndrome, with severe hypoxia and high mortality risk.¹ Early identification of patients who will develop severe respiratory insufficiency is of pivotal importance.

Chest computed tomography (CT) is widely performed in the current SARS-CoV-2 outbreak to diagnose COVID-19 pneumonia, especially in overwhelmed emergency departments (ED) to streamline clinical decision-making.^{2,3} On CT, COVID-19 pneumonia shows typical features of interstitial inflammatory disease, including ground glass opacities (GGO), semi-consolidation components and consolidation.⁴ These features reflect the different stages and severity of pathologic alteration of the lungs. GGO presents as a mild increased attenuation in the lung due to incomplete air filling of alveolar cavity, with mild thickening of the alveolar walls and interstitium.⁵ Progressive filling of the alveolar cavity, with greater degree of alveolar wall and interstitial septal thickness, leads to semi-consolidation, with possible superimposed reticular crazy paving pattern. Finally, complete air space filling results in consolidation on CT scan.^{6–9}

Qualitative and semiquantitative scores were developed for initial assessment^{10,11} and follow-up^{12,13} in COVID-19 pneumonia, but are potentially subject to intra- and inter-observer variability, due to their subjective nature.¹⁴

Quantitative analysis of CT images allows to extract the percentage of lung parenchyma volume involved by pneumonia with an automatic approach based on Hounsfield Units (HU) values.^{14,15}

In COVID-19 patients, pneumonia features likely impact on respiratory system compliance¹⁶ representing different stages and degrees of severity of pathophysiological process. Therefore, they may also potentially impact on response to therapies.

Hence, a quantitative assessment of lung involvement, based on pixel densities, may have a pivotal role in determining the risk of developing severe hypoxia and critical course of the disease. Therefore, the aim of the present study was to define the predictive value of quantitative features of COVID-19 pneumonia, extracted by chest CT scans acquired at hospital admission, on patients' hypoxia during hospitalization and on outcome.

2. Materials and methods

2.1. Study population

This study was approved by the Institutional Review Board (IRB approval number 67/INT/2020) and the informed consent was waived. We included consecutive patients referred to the emergency department of San Raffaele hospital of Milan, in North Italy,¹⁷ between March 1st and April 7th, 2020, in whom a CT scan was performed within 24 h from hospital admission for clinical suspicion of COVID-19 pneumonia (Fig. 1), but with inconclusive or possible false-negative X-ray results, according to national recommendation.¹⁸

Results from RT-PCR on nasopharyngeal swabs were collected in all patients, as number of swabs performed, turnaround time and time-to-positive results.

We excluded patients with: 1) negative chest CT, 2) repeated negative RT-PCR for SARS-CoV-2, 3) low quality CT scan for breathing artifacts, 4) contrast-enhanced CT examinations (Fig. 1).

Demographics, laboratory and clinical data including symptoms, symptoms duration, and comorbidities were reported. Moreover worst O₂ pressure (pO₂) at hemogasanalysis during the hospitalization, length of hospital stay and death were collected.

2.2. CT scan protocol

All CT scans for suspected COVID-19 pneumonia was performed in a dedicated suite easily accessible from emergency department via assigned elevators and paths.

Chest CT scans were performed on a 64-slice scanner (LightSpeed VCT, GE Healthcare) in supine position, during inspiratory breath hold. CT scan parameters were as follows: 120 kV tube voltage, 150–550 mA automatic tube current modulation, 0.4 s rotation time, pitch of 1.375 mm/rot, 64 × 0.625 mm detector collimation. Images were reconstructed at slice thickness/interval of 1.25 mm with a hybrid adaptive statistical iterative reconstruction (40% level) using bone/lung plus kernels (GE Healthcare) and lung window width/level 1500/-700HU. The mean DLP was 478 ± 184 mGy·cm.

Qualitative analysis was performed according to RSNA Expert Consensus document.⁴ Presence of fibrosis, emphysema, lymph adenomegaly and pleural effusion was assessed.

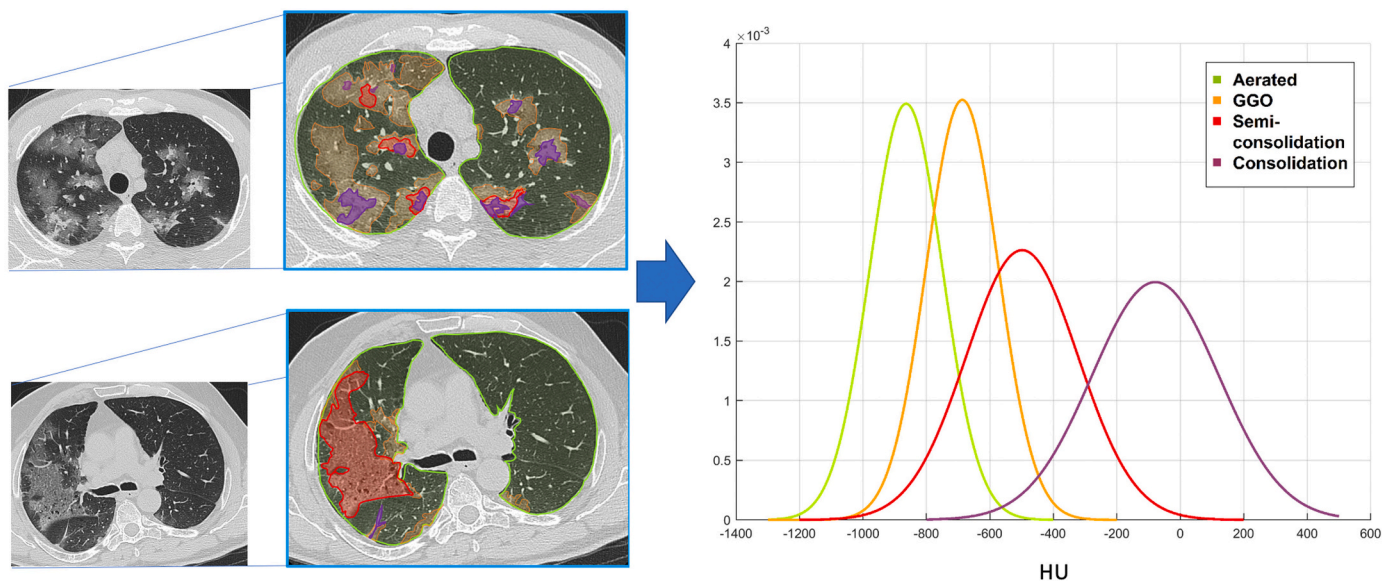


Fig. 2. HU density values extraction. An experienced radiologist segmented the well-aerated parenchyma (lime), ground glass opacities (orange), semi-consolidation (red) and consolidation (plum) on chest CT scan of a subset of 35 randomly selected patients with COVID-19 pneumonia. Two examples of manual segmentation are reported on the left. HU values of each pneumonia lesion features and well-aerated parenchyma were extracted using a pixel-by-pixel approach and Gaussian curves of HU values distribution were created (on the right). Intersection points of Gaussian curves identified the following HU threshold values: - 780 HU as threshold between well-aerated parenchyma and GGO; -570 HU as threshold between GGO and semi-consolidation; -290 as threshold between semi-consolidation and consolidation. (For interpretation of the references to color in this figure legend, the reader is referred to the web version of this article.)

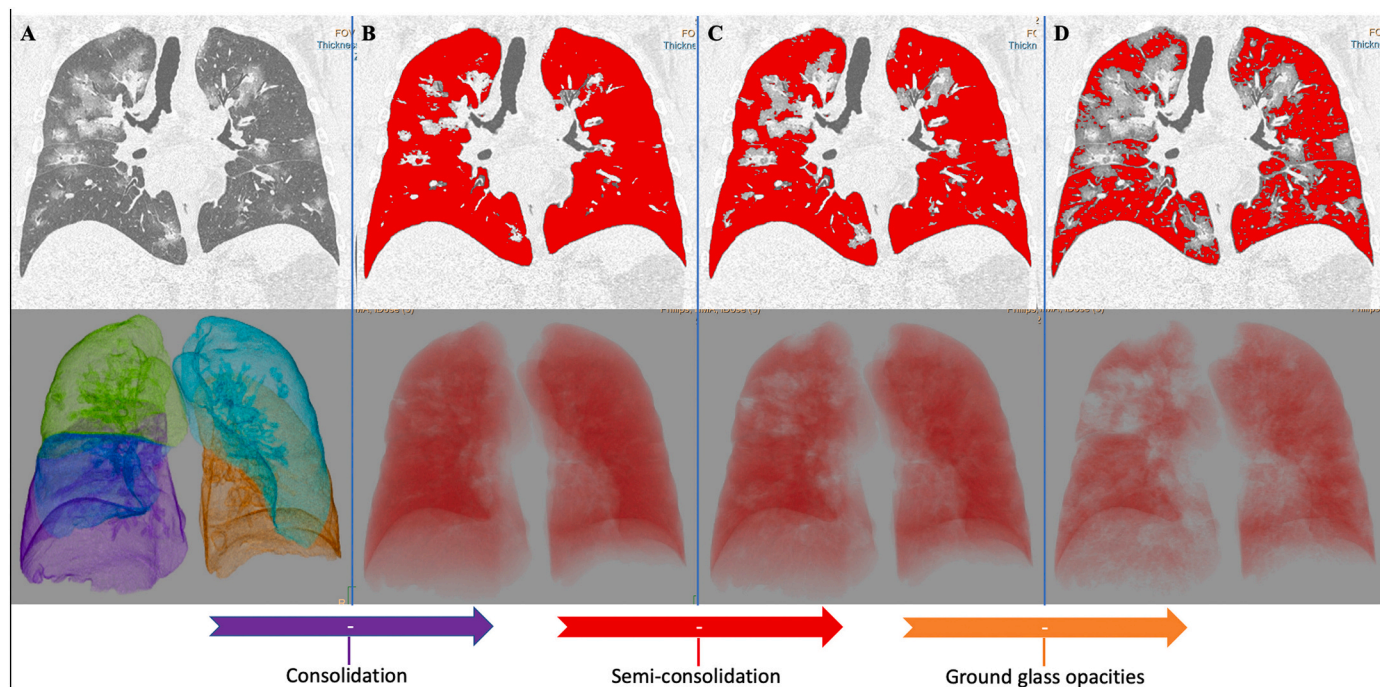


Fig. 3. Automatic segmentation of both lungs with quantitative extraction of well-aerated parenchyma, ground glass opacities, semi-consolidation and consolidation. This figure reports the coronal images (on top) and the corresponding 3D volume rendering (bottom), obtained during post-processing performed using a dedicated software (IntelliSpace Portal v.8.0, Philips Medical Systems, Eindhoven, The Netherlands). The software performs a fully automatic segmentation of both lungs from native CT dataset (A). After visual check and manual correction of any segmentation error, the HU thresholds calculated as in Fig. 2 were applied in a multistep fashion analysis. In the first step (B) consolidation pattern was extracted from total lung volume applying the threshold -290HU. In the second step (C) consolidation plus semi-consolidation were extracted from total lung volume applying the threshold -570HU. In the final step (D) consolidation, semi-consolidation and ground glass opacities were extracted from total lung volume applying the threshold -780HU and the red volume (D) represent the well-aerated parenchyma. Hence, consolidation volume was obtained subtracting red volume in B from total lung volume (A); semi-consolidation volume was obtained subtracting red volume in C from red volume in B; ground glass volume was obtained subtracting red volume in D from red volume in C. (For interpretation of the references to color in this figure legend, the reader is referred to the web version of this article.)

2.3. Image analysis: threshold values identification

The chest CT scans of 35 randomly selected patients were manually segmented by an experienced radiologist (AP with 9 years of experience in chest imaging) in order to identify the threshold density values for each of pneumonia features. Volumes of Interest (VOIs) for well-aerated lung parenchyma, GGO, semi-consolidation and consolidation were depicted. The histograms of HU distribution within each VOIs were extracted. Then, data fitting was performed with ad-hoc function using MATLAB® (R2017b, The MathWorks Inc., Natick, Massachusetts, USA). Normal probability distribution was created to fit each CT feature of lung involvement.

Mean HU values for each lung feature were obtained as -864 ± 114 for well-aerated lung, -687 ± 116 for GGO, -498 ± 210 for semi-consolidation and -78 ± 343 for consolidation (Fig. 2). Intersection points of Gaussian curves were: -780 HU as threshold between well-aerated parenchyma and GGO; -570 HU as threshold between GGO and semi-consolidation; -290 as threshold between semi-consolidation and consolidation (Fig. 2).

Intersection points of Gaussian curves of CT attenuation pattern were used to define HU threshold values for the automatic segmentation in the entire population.

2.4. Image analysis: automatic lung components segmentation and quantification

Quantitative analysis was performed using a dedicated software (IntelliSpace Portal v.8.0, Philips Medical Systems, Eindhoven, The Netherlands).

After a fully automatic segmentation of both lungs, the segmentation errors were manually corrected by an experienced radiologist. Then, the volume and the percentage of well-aerated lung and of each pneumonia features (GGO, semi-consolidation and consolidation) were extracted using the aforementioned HU thresholds values, as follows: well-aerated parenchyma < -780 HU, GGO ≥ -780 HU < -570 HU, semi-consolidation ≥ -570 HU < -290 HU, consolidation ≥ -290 HU (Fig. 3).

Considering the variability of lung volume depending on patients' age, body size and degree of inspiration, the extension of the four different quantitative parameters of lung involvement was expressed as percentage of the entire lung volume in order to ensure a more robust evaluation.

2.5. Statistical analysis

Spearman correlation coefficient was used for evaluating correlations between numerical variables. Associations between binary variables were evaluated with Fisher exact test. Comparison of numerical variables between two or more groups were performed with Mann-Whitney or Kruskal-Wallis test, respectively. When needed, post-hoc comparisons of Kruskal-Wallis test were performed with Dunn test. In all analyses involving multiple testing or comparisons, *p*-values were adjusted with Bonferroni correction. The receiver operating characteristics (ROC) curve analysis was used to assess the performance of CT pneumonia components in predicting severe hypoxia or discharged vs. dead patients. According to Hosmer DW¹⁹ the values of the Area Under the ROC Curve (AUC) were interpreted as: 0.7–0.8 acceptable, 0.8–0.9 excellent, >0.9 outstanding. The optimal cut-off of each variable was found as the value minimizing the Euclidean distance of the corresponding point on the ROC curve with the upper left corner of the ROC plane. Sensitivity, specificity and accuracy were calculated for each parameter categorized with the optimal cut-off. Multiple Cox proportional hazards regression was used to predict the time to discharge, depending on the CT parameters, demographic and clinical variables (sex, age, time from first symptoms, SatO₂, pO₂, comorbidities). Patients still hospitalized at the time of the analysis or dead were considered as censored data in the analysis. Final models were obtained with

Table 1

Clinical, demographics and CT qualitative features of the study population.

	Overall (n = 77)
Age, y.o.	56 [IQR, 48–71]
Sex, M	51
Comorbidities	
Cardiovascular	38 (49%)
Respiratory	4 (5%)
Oncological	14 (18%)
Neurological	3 (4%)
Chronic kidney failure	1 (1%)
Obesity	7 (9%)
Immunodepression	5 (6%)
Diabetes	15 (19%)
Symptoms, n (%)	
Fever	72 (94%)
Cough	45 (58%)
Dyspnea	22 (29%)
Asthenia	6 (8%)
Diarrhea	4 (5%)
Other	8 (10%)
Symptom onset, days	7 [IQR, 4–10]
White blood count, $\times 10^9/L$	6 [IQR, 4.68–8.68]
Lymphocyte count, $\times 10^9/L$	1.2 [IQR, 0.8–16.7]
CRP, mg/L	2.1 [IQR, 0.85–3.9]
Body temperature, °C	38 [IQR, 37.5–39]
O ₂ Saturation, %	93 [IQR, 89–96]
CT features	
CT typical pattern, n (%)	69 (90%)
CT indeterminate pattern, n (%)	5 (6%)
CT atypical pattern, n (%)	3 (4%)
Peripheral distribution, n (%)	74 (96%)
> 3 lobes involved, n (%)	68 (88%)
Pulmonary fibrosis, n (%)	7 (9%)
Lymph adenomegaly, n (%)	20 (26%)
Pleural effusion, n (%)	5 (6%)
Emphysema, n (%)	6 (8%)

backward variable selection. *p*-Values less than 0.05 were considered significant. All confidence intervals were computed at 95% confidence level. Statistical analyses were performed using R3.5.0 (<http://www.R-project.org/>).

3. Results

3.1. Patient characteristics

The final cohort consisted of 77 patients (median age:56 y.o. [IQR, 48–71 y.o.]), mainly men (51/77, 66%). Most of patients (72/77 94%) had fever on admission (median 38 °C [IQR, 37.5–39 °C] from a median of 7 days [IQR, 4–10]), together with cough (45/77, 58%) and/or dyspnea (22/77, 29%) with median oxygen saturation (SatO₂) of 93% [IQR, 89–96%] and median pO₂ of 65 mm Hg [IQR, 56–74 mm Hg].

Forty-seven patients (61%) suffered from comorbidities, mostly cardiovascular disease (*n* = 38) and active cancer (*n* = 14), twenty-seven (35%) had multiple comorbidities. Three patients were rapidly discharged (within 3 days from admission) and addressed to home care. The remaining 74 patients were hospitalized for 14 days [IQR, 9–26 days]; 14 patients were still hospitalized at the time of analysis and 12 patients died. Demographics, clinical, laboratory findings and CT qualitative features at admission are reported in Table 1.

3.2. Lung involvement at quantitative CT according to demographics and clinical parameters

Bilateral total lung volume at the admission CT scan was 3347 cc [IQR, 2776–4329 cc] with median pneumonia involvement of 42% [IQR, 29–55%] of lung parenchyma. Semi-consolidation was the main pneumonia feature (median 17% [IQR, 11–26%]), followed by GGO (median 11% [IQR, 8–13%]) and consolidation (median 9% [IQR,

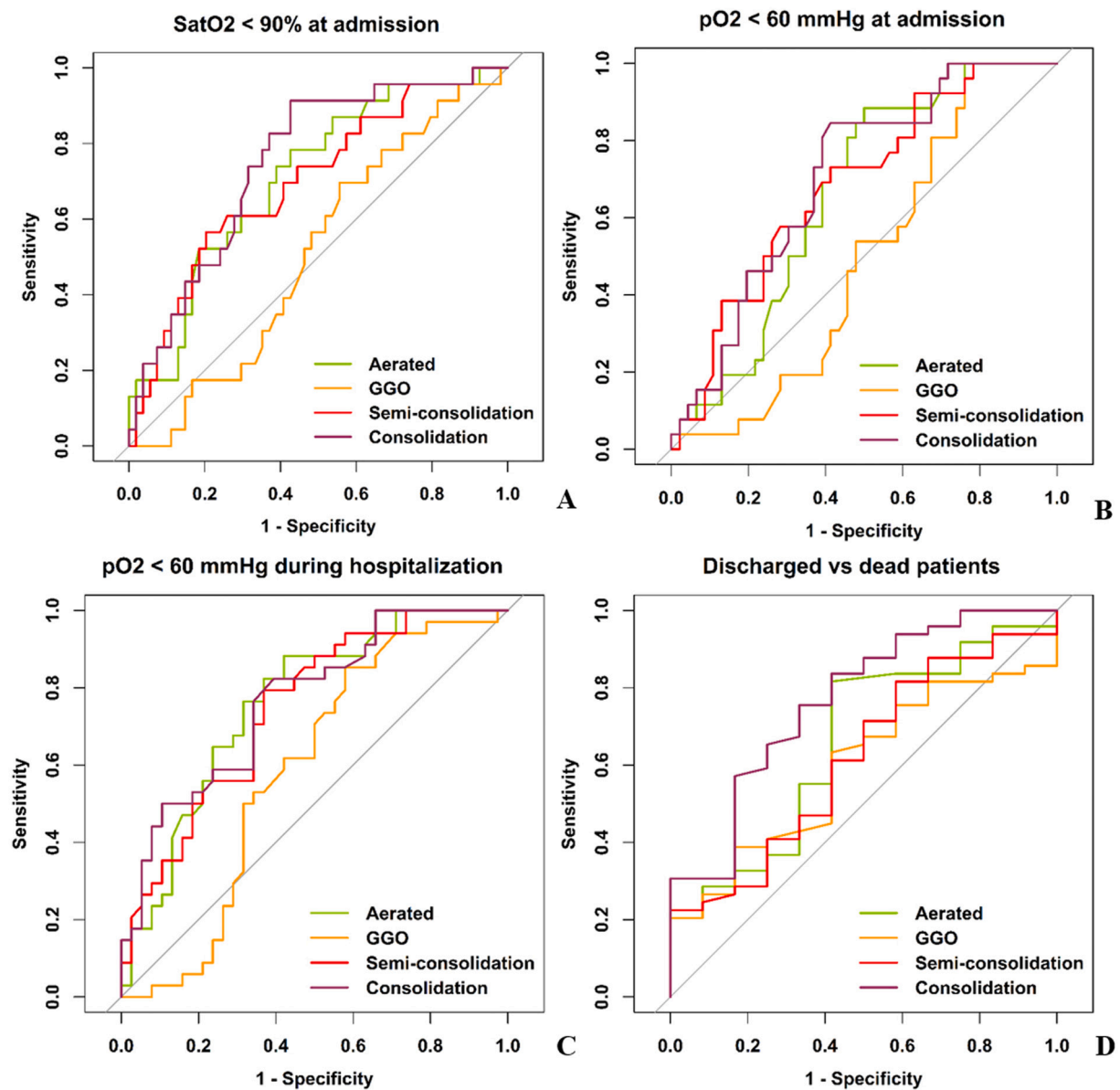


Fig. 4. ROC curves of CT quantitative features of lung involvement in patients' suffering from COVID-19 pneumonia in predicting oxygen saturation (A), hypoxemia at hospital arrival (B) and during hospitalization (C) and patients' outcome (D). GGO had the worst AUCs, and was found as predictor neither of oxygen saturation (AUC 0.51), hypoxemia at time of admission (AUC 0.51) and during the hospitalization (AUC 0.59) nor of patients' outcome (AUC 0.59).

6–15%]).

The quantitative extension of each pneumonia feature was not significantly correlated to age, sex (Fig. A1 and Table A1) and time-from-symptoms onset (Fig. 4A and Table A1).

Lung involvement was correlated to the number of comorbidities: more comorbidities were associated to lower well-aerated parenchyma ratio ($\rho = -0.234$, $p = 0.04$), and higher semi-consolidation ratio ($\rho = -0.303$, $p = 0.008$) (Table A1 and Fig. 4B).

Well-aerated parenchyma, semi-consolidation and consolidation were all associated with lymphocyte count and C-reactive protein (CRP). Well-aerated parenchyma directly correlated to lymphocyte ($\rho = 0.295$, $p = 0.01$) and inversely correlated to CRP ($\rho = -0.292$, $p = 0.01$). Conversely, semi-consolidation and consolidation ratio were inversely correlated to lymphocyte ($\rho = -0.316$, $p = 0.006$ and $\rho = -0.297$, $p = 0.001$, respectively) and directly to CRP ($\rho = 0.265$, $p = 0.02$ and $\rho = -0.443$, $p < 0.001$, respectively).

Notably, GGO was not correlated to lymphocyte ($\rho = -0.091$, $p = 0.436$) and CRP ($\rho = -0.025$, $p = 0.828$) (Table A1).

3.3. Quantitative lung involvement at CT and hypoxia

Lung involvement varied according to SatO₂ and pO₂ measured at patients' arrival at the emergency department (Fig. 4 and Table A2).

Well-aerated parenchyma ratio, semi-consolidation and consolidation ratio correlated both with SatO₂ ($\rho = 0.364$, $p = 0.001$; $\rho = -0.388$, $p < 0.001$; $\rho = -0.448$, $p < 0.001$, respectively) and with pO₂ ($\rho = 0.249$, $p = 0.034$; $\rho = -0.306$, $p = 0.009$; $\rho = -0.373$, $p = 0.001$, respectively).

However, a post-hoc analysis comparing different classes of hypoxia (SatO₂ $\geq 94\%$; SatO₂ = 90–93%; SatO₂ < 90%) demonstrated that only semi-consolidation ($p < 0.01$) and consolidation ratio ($p < 0.01$) were significantly different between patients with SatO₂ ≥ 94 and SatO₂ < 90% (Fig. 4C and D).

Consolidation ratio was significantly different ($p = 0.01$) also between patients with severe hypoxemia (pO₂ < 60 mm Hg) and normoxemia (pO₂ > 80 mm Hg) at the initial hemogasanalysis.

GGO ratio was correlated with neither SatO₂ nor pO₂ ($\rho = -0.036$,

Table 2

ROC curves of quantitative parameters of lung involvement on CT at hospital admission in the prediction of patients' hypoxia and hospital discharging.

Parameters	AUC ^a	Cut-off	Sensitivity ^b	Specificity ^b	Accuracy ^b
SatO2 < 90% at admission					
Aerated lung ratio	0.71 (0.58,84)	≤57	16/23 (70) [47,87]	33/54 (61) [47,74]	49/77 (64) [52,74]
GGO ratio	0.51 (0.37,0.65)	≥10	16/23 (70) [47,87]	24/54 (44) [31,59]	40/77 (52) [40,63]
Semi-consolidation ratio	0.70 (0.56,0.83)	≥23	13/23 (57) [34,77]	43/54 (80) [66,89]	56/77 (73) [61,82]
Consolidation ratio	0.75 (0.62,0.88)	≥11	16/23 (70) [47,87]	37/54 (69) [54,80]	53/77 (69) [57,79]
pO2 < 60 mm Hg at admission					
Aerated lung ratio	0.66 (0.53,0.80)	≤57	18/26 (69) [48,86]	27/46 (59) [43,73]	45/72 (62) [50,74]
GGO ratio	0.51 (0.37,0.65)	≥12	13/26 (50) [30,70]	24/46 (52) [37,67]	37/72 (51) [39,63]
Semi-consolidation ratio	0.68 (0.55,0.82)	≥17	18/26 (69) [48,86]	28/46 (61) [45,75]	46/72 (64) [52,75]
Consolidation ratio	0.70 (0.57,0.83)	≥9	20/26 (77) [56,91]	28/46 (61) [45,75]	48/72 (67) [55,77]
pO2 < 60 mm Hg during hospitalization					
Aerated lung ratio	0.76 (0.65;0.87)	≤57	25/34 (74) [56,87]	26/38 (68) [51,82]	51/72 (71) [59,81]
GGO ratio	0.59 (0.45;0.72)	≥12	17/34 (50) [32,68]	25/38 (66) [49,80]	42/72 (58) [46,70]
Semi-consolidation ratio	0.75 (0.63;0.86)	≥17	24/34 (71) [53,85]	25/38 (66) [49,80]	49/72 (68) [56,79]
Consolidation ratio	0.77 (0.65;0.88)	≥9	25/34 (74) [56,87]	25/38 (66) [49,80]	50/72 (69) [57,80]
ROC curve analysis predicting discharged vs dead patients					
Aerated lung ratio	0.66 (0.50;0.82)	≥45	40/49 (82) [68,91]	7/12 (58) [28,85]	47/61 (77) [65,87]
GGO ratio	0.59 (0.42;0.77)	≤10	30/49 (61) [46,75]	7/12 (58) [28,85]	37/61 (61) [47,73]
Semi-consolidation ratio	0.62 (0.45;0.79)	≤17	30/49 (61) [46,75]	7/12 (58) [28,85]	37/61 (61) [47,73]
Consolidation ratio	0.77 (0.64;0.90)	≤13	36/49 (73) [59,85]	8/12 (67) [35,90]	44/61 (72) [59,83]

GGO: ground glass opacity, SatO2: oxygen saturation, pO2: oxygen pressure.

^a Data in parentheses are 95% confidence intervals (CIs).

^b Data are numerators and denominators, with percentages in parentheses. Data in brackets are 95% CIs.

Table 3

Clinical, demographic and CT features in dead and discharged patients

	Dead (n = 12)	Discharged (n = 49)	p value
Sex, M	9 (75%)	34 (69%)	1.00
Age, years-old	74 [69;81]	53 [47;67]	0.001
Time from symptoms, days	7 [2;7]	7 [5;10]	1.00
SatO2 at admission, %	90 [86;95]	94 [90;96]	1.00
pO2 at admission, mm Hg	59 [48;73]	65[59;74]	1.00
Worst pO2 during hospitalization, mm Hg	47 [36;56]	65 [58;70]	<0.001
Comorbidities, n°	2 [1;4]	1 [0;2]	0.027
Aerated lung, %	45 [38;69]	62 [51;77]	0.898
GGO, %	9 [7;12]	11 [8;14]	1.00
Semi-consolidation, %	20 [13;28]	16 [9;23]	1.00
Consolidation, %	16 [11;26]	7 [4;13]	0.047

GGO: ground glass opacity, SatO2: oxygen saturation, pO2: oxygen pressure.

Table 4

Multiple Cox's regression analysis including clinical, demographic and CT quantitative parameters of lung involvement for predicting patients' discharge

Variables	Aerated lung ratio		GGO ratio		Semi-consolidation ratio		Consolidation ration		With all CT parameters	
	HR (95% CI)	p value	HR (95% CI)	p value	HR (95% CI)	p value	HR (95% CI)	p value	HR (95% CI)	p value
sex M vs F	0.24 (0.11–0.51)	<0.001	0.38 (0.20–0.72)	<0.01	0.37 (0.19–0.71)	<0.01	0.32 (0.16–0.62)	<0.001	0.26 (0.13–0.55)	<0.001
Age, y.o.	0.97 (0.95–0.99)	<0.01	–	–	0.97 (0.95–0.99)	0.02	0.97 (0.95–0.99)	<0.01	0.97 (0.94–0.99)	<0.01
Time from symptoms onset	1.07 (1.01–1.14)	0.03	–	–	–	–	–	–	1.06 (1.01–1.12)	0.049
SatO2, %	–	–	1.02 (1.02–1.15)	<0.01	–	–	–	–	–	–
Neoplasia	–	–	0.32 (0.13–0.83)	0.02	–	–	0.39 (0.15–0.99)	0.049	–	–
Aerated lung ≥ 45%	3.93 (1.73–8.92)	<0.01	–	–	–	–	–	–	–	–
CP ≤ 17%	–	–	–	–	3.32 (1.76–6.27)	<0.001	–	–	2.60 (1.32–5.11)	<0.01
Consolidation ≤ 13%	–	–	–	–	–	–	3.42 (1.68–6.97)	<0.001	2.36 (1.12–5.00)	0.03

GGO: ground glass opacity, SatO2: oxygen saturation, pO2: oxygen pressure, HR: Hazard ratio, CI: Confidence Interval.

$p = 0.756$ and $\rho = -0.064$, $p = 0.596$ respectively) (Table A1).

ROC curves in Fig. 4A–B showed that well-aerated parenchyma, semi-consolidation and consolidation were moderately associated with hypoxia at hospital arrival (SatO2 < 90% and pO2 < 60%), while GGO showed no association (Table 2). Similarly, well-aerated parenchyma, semi-consolidation and consolidation predicted severe hypoxia during hospitalization with moderate AUC (76%, 75% and 77%, respectively), while GGO was not found as a predictor. (Fig. 4C, Table 2).

3.4. Quantitative lung involvement at admission CT and patients' outcome

Non-survivors were mainly men (9/12, 75%) with older age compared to survivors (74 [69–81] years vs. 53 [47–67] years, $p < 0.01$) (Table 3), mostly suffering from multiple comorbidities (7/12, 58%).

At ROC curve analysis for predicting patients' survival (Fig. 4D and Table 2) based on pneumonia quantitative features at admission, GGO showed no role (AUC 0.59, sensitivity 61%, specificity 58%, accuracy 61%), differently from well-aerated lung ($\geq 45\%$), semi-consolidation ($\leq 17\%$) and consolidation ($\leq 13\%$) which demonstrated performances

ranging from acceptable to good (AUC 0.66, 0.62 and 0.77, respectively).

A time-to-event multiple Cox regression analysis with the hospital discharge defined as the event, showed that well-aerated parenchyma $\geq 45\%$ ($p < 0.01$), semi-consolidation $\leq 17\%$ ($p < 0.001$) and consolidation $\leq 13\%$ ($p < 0.001$) predicted a reduced time to discharge (Table 4). Male sex and age predicted a longer time to discharge.

At multiple Cox regression analysis evaluating the role of all four CT quantitative parameters of lung involvement evaluated at hospital admission together with demographic and clinical variables, lower age ($p < 0.01$), female sex ($p < 0.001$), longer time-from-symptoms onset ($p = 0.049$), semi-consolidation $\leq 17\%$ ($p < 0.01$) and consolidation $\leq 13\%$ ($p = 0.03$) significantly predicted a shorter time to discharge (Table 4).

4. Discussion

In the setting of COVID-19 outbreak, risk assessment for a tailored patients' management is of pivotal importance.

Recent study showed that well-aerated lung parenchyma ratio predicted the admission to intensive care unit and death.²⁰ However, in COVID-19 interstitial pneumonia, as in other types of interstitial lung disease, it is expected that HU values of pneumonia lesions might depict different degrees of severity of lung damage,^{5,9} which subsequently impact on respiratory function and potentially on disease course and severity.

The aim of the present study was to quantify the lung involvement in COVID-19 patients including pneumonia lesions based on different CT densities, in order to evaluate their impact on patients' hypoxia at time of admission and during hospitalization, as well as on patients' outcome.

In our analysis of patients referred to emergency department for COVID-19 pneumonia, the following results were observed: i) COVID-19 pneumonia CT findings at hospital admission did not differ with age, sex and time-from-symptoms onset, while significantly changed with number of patients' comorbidity: higher number of comorbidities was associated to lower well-aerated parenchyma ratio and increased semi-consolidation ratio, ii) GGO ratio was neither associated with oxygen saturation and hypoxemia at the admission nor with the occurrence of severe hypoxia during hospitalization, differently from semi-consolidation, consolidation, and well-aerated parenchyma ratio, iii) at multiple Cox regression analysis evaluating the role of all quantitative CT parameters of lung involvement together with demographic and clinical variables, semi-consolidation $\leq 17\%$ ($p < 0.01$) and consolidation $\leq 13\%$ ($p = 0.02$) significantly predicted a shorter time to hospital discharge with younger age ($p < 0.01$), female sex ($p < 0.001$) and longer time-from-symptoms ($p = 0.049$).

In our cohort, age and sex showed no significant impact on the lung lesion extension and density. Pneumonia features quantified based on CT attenuation threshold demonstrated no significant difference according to time-from-symptoms onset, different from the previously reported data.^{12,21} These findings suggest potentially different disease progression kinetics among patients or presence of a selection bias (i.e. only patients referred to the emergency department were included in the study).

In accordance with previous literature,²² higher burden of disease was observed in patients with multiple comorbidities.

Semi-consolidation was the main component of pneumonia independently from clinical and demographic parameters.

Despite a certain degree of HU values overlap among pneumonia features, it was revealed that the prevalence of pneumonia pattern with intermediate density (semi-consolidation, from -570 HU to -290 HU) was a predictor of hypoxia and outcome, similarly to consolidated parenchyma. This finding suggests that in COVID-19 pneumonia, semi-consolidation might represent a severe stage of endothelial damage²³ in which despite the persistence of air filling, a significant impairment of gas exchange occurs. Furthermore, it can explain the higher compliance but the worst oxygenation observed in COVID-19 acute respiratory

distress syndrome (ARDS) compared to non-COVID-19 ARDS.¹⁶

On contrary, pure GGO component demonstrated no significant correlation with lab tests and no role in prediction of hypoxia and outcome. Thus, it can be suggested that in case of pure GGO involving 10–12% of lung volume, a mild damage without significant impact on systemic condition or respiratory function occurs.

This result may explain previous evidence of GGO as the predominant feature in asymptomatic^{24,25} and pauci-symptomatic COVID-19 patients.²¹ In fact, despite the similar percentage of lung involvement by GGO and consolidation (11 [8–13] vs. 9 [6–15] %), the GGO density suggested a mild damage. In fact in our cohort, GGO was identified by HU values ranging between -780 HU (indicating lung lesion consisting in nearly 80% gas and 20% tissue) and -570 HU (indicating nearly 60% gas and 40% tissue), suggestive for mild lung damage. On the contrary, consolidation was identified by HU values higher than -290 , indicating a volume of lung occupied by air for less than 30%.

Our results are in agreement with the only previous study assessing the relation between three quantitative features of COVID-19 pneumonia and patients' outcome on a Chinese population.²⁶ Similarly to Liu et al., we found a moderate performance of baseline CT features to early predict patients' outcome. However, to the best of our knowledge, this result was never confirmed on population outside China before our study. Additionally, in the present study we assessed also the association of quantitative pneumonia features measured on admitting chest CT with respiratory function at the admission and during hospitalization.

In accordance with previous study in non-COVID ARDS²⁷ and critical COVID-19 pneumonia,²⁴ well-aerated parenchyma ratio near 40% ($\leq 45\%$) predicted unfavorable outcome.

The Cox regression analysis accounting for all CT pneumonia features, demographic and clinical parameters, confirmed the prognostic value of pneumonia features except for GGO.

Our results provide a new insight in the capability of chest CT to characterize COVID-19 pneumonia, highlighting an association between the pneumonia density and hypoxia. These data could further expand the capability of CT to characterize the different pathophysiological features involved in COVID-19 pneumonia behind the extension of lung involvement, together with the assessment of thromboembolic complication²⁸ and cardiovascular implication.^{29,30}

Our data need to be confirmed on a larger sample and to be correlated to therapeutic options.

5. Conclusion

Semi-consolidation and consolidation at admitting CT are associated to hypoxia and played a significant role in the prediction of hypoxia worsening during hospitalization.

Quantification of pneumonia features may contribute to timely stratify patients' risk if combined with demographic, clinical and lab parameters, potentially improving patients' care.^{16,31} This could help clinical decision making and may potentially improve resource allocation, especially in overwhelmed conditions.

Acknowledgment

We would like to thank Dr. Fatemeh Darvizeh for careful editing the language of our manuscript.

Appendix A. Supplementary data

Supplementary data to this article can be found online at <https://doi.org/10.1016/j.clinimag.2021.04.033>.

References

- [1] Matthay MA, Aldrich JM, Gotts JE. Treatment for severe acute respiratory distress syndrome from COVID-19. *Lancet Respir Med* 2020 May 1;8(5):433–4.

- [2] Ai T, Yang Z, Hou H, et al. Correlation of chest CT and RT-PCR testing in coronavirus disease 2019 (COVID-19) in China: a report of 1014 cases. *Radiology*. 2020 Feb;26:200642.
- [3] Palmisano A, Scotti GM, Ippolito D, et al. Chest CT in the emergency department for suspected COVID-19 pneumonia. *Radiol Med (Torino)* 2020 Nov;9:1–5.
- [4] Simpson S, Kay FU, Abbara S, et al. Radiological society of North America expert consensus document on reporting chest CT findings related to COVID-19: endorsed by the society of thoracic radiology, the American college of radiology, and RSNA. *Radiol Cardiothorac Imag* 2020 Mar 25;2(2):e200152.
- [5] Remy-Jardin M, Giraud F, Remy J, Copin MC, Gosselin B, Duhamel A. Importance of ground-glass attenuation in chronic diffuse infiltrative lung disease: pathologic-CT correlation. *Radiology*. 1993 Dec;189(3):693–8.
- [6] Tian S, Hu W, Niu L, Liu H, Xu H, Xiao S-Y. Pulmonary pathology of early-phase 2019 novel coronavirus (COVID-19) pneumonia in two patients with lung cancer. *J Thorac Oncol Off Publ Int Assoc Study Lung Cancer* 2020;15(5):700–4.
- [7] Franquet T. Imaging of pulmonary viral pneumonia. *Radiology*. 2011 Jul;260(1):18–39.
- [8] Xu Z, Shi L, Wang Y, et al. Pathological findings of COVID-19 associated with acute respiratory distress syndrome. *Lancet Respir Med* 2020;8(4):420–2.
- [9] De Wever W, Meerschaert J, Coolen J, Verbeke E, Verschakelen JA. The crazy-paving pattern: a radiological-pathological correlation. *Insights Imaging* 2011 Apr;2(2):117–32.
- [10] Yang R, Li X, Liu H, et al. Chest CT severity score: an imaging tool for assessing severe COVID-19. *Radiol Cardiothorac Imaging* 2020 Mar 30;2(2):e200047.
- [11] Li K, Fang Y, Li W, et al. CT image visual quantitative evaluation and clinical classification of coronavirus disease (COVID-19). *Eur Radiol* 2020 Aug;30(8):4407–16.
- [12] Pan F, Ye T, Sun P, et al. Time course of lung changes on chest CT during recovery from 2019 novel coronavirus (COVID-19) pneumonia. *Radiology*. 2020 Feb;13:200370.
- [13] Wang Y, Dong C, Hu Y, et al. Temporal changes of CT findings in 90 patients with COVID-19 pneumonia: a longitudinal study. *Radiology*. 2020 Mar;19:200843.
- [14] Huang L, Han R, Ai T, et al. Serial quantitative chest CT assessment of COVID-19: deep-learning approach. *Radiol Cardiothorac Imaging* 2020 Mar 30;2(2):e200075.
- [15] Zhang K, Liu X, Shen J, et al. Clinically applicable AI system for accurate diagnosis, quantitative measurements, and prognosis of COVID-19 pneumonia using computed tomography. *Cell*. 2020 Jun 11;181(6):1423–33.
- [16] Chiumello D, Busana M, Coppola S, et al. Physiological and quantitative CT-scan characterization of COVID-19 and typical ARDS: a matched cohort study. *Intensive Care Med* 2020 Dec 1;46(12):2187–96.
- [17] Zangrillo A, Beretta L, Silvani P, et al. Fast reshaping of intensive care unit facilities in a large metropolitan hospital in Milan, Italy: facing the COVID-19 pandemic emergency. *Crit Care Resusc* 2020 Jun;22(2):91.
- [18] Neri E, Miele V, Coppola F, Grassi R. Use of CT and artificial intelligence in suspected or COVID-19 positive patients: statement of the Italian Society of Medical and Interventional Radiology. *Radiol Med (Torino)* 2020 May;125(5):505–8.
19. Hosmer DW. *Applied Logistic Regression*, 3rd Edition |Wiley.com.
- [20] Colombi D, Bodini FC, Petrini M, et al. Well-aerated lung on admitting chest CT to predict adverse outcome in COVID-19 pneumonia. *Radiology*. 2020 Apr;17:201433.
- [21] Shi H, Han X, Jiang N, et al. Radiological findings from 81 patients with COVID-19 pneumonia in Wuhan, China: a descriptive study. *Lancet Infect Dis* 2020;20(4):425–34.
- [22] Richardson S, Hirsch JS, Narasimhan M, et al. Presenting characteristics, comorbidities, and outcomes among 5700 patients hospitalized with COVID-19 in the New York City area. *JAMA*. 2020 May 26;323(20):2052–9.
- [23] Varga Z, Flammer AJ, Steiger P, et al. Endothelial cell infection and endothelitis in COVID-19. *Lancet Lond Engl* 2020;395(10234):1417–8. 02.
- [24] Inui S, Fujikawa A, Jitsu M, et al. Chest CT findings in cases from the cruise ship “diamond princess” with coronavirus disease 2019 (COVID-19). *Radiol Cardiothorac Imaging* 2020 Mar 17;2(2):e200110.
- [25] Zeng Y, Fu J, Yu X, et al. Should computed tomography (CT) be used as a screening or follow-up tool for asymptomatic patients with SARS-CoV-2 infection? *Quant Imaging Med Surg* 2020 May;10(5):1150–2.
- [26] Liu F, Zhang Q, Huang C, et al. CT quantification of pneumonia lesions in early days predicts progression to severe illness in a cohort of COVID-19 patients. *Theranostics*. 2020;10(12):5613.
- [27] Nishiyama A, Kawata N, Yokota H, et al. A predictive factor for patients with acute respiratory distress syndrome: CT lung volumetry of the well-aerated region as an automated method. *Eur J Radiol* 2020 Jan;122:108748.
- [28] Loffi M, Regazzoni V, Toselli M, et al. Incidence and characterization of acute pulmonary embolism in patients with SARS-CoV-2 pneumonia: a multicenter Italian experience. *PLoS One* 2021;16(1):e0245565.
- [29] Esposito A, Palmisano A, Toselli M, et al. Chest CT-derived pulmonary artery enlargement at the admission predicts overall survival in COVID-19 patients: insight from 1461 consecutive patients in Italy. *Eur Radiol* 2020 Dec;23:1–11.
- [30] Pontone G, Baggiano A, Conte E, et al. “Quadruple rule-out” with computed tomography in a COVID-19 patient with equivocal acute coronary syndrome presentation. *JACC Cardiovasc Imaging* 2020;13(8):1854–6.
- [31] Huang G, Gong T, Wang G, et al. Timely diagnosis and treatment shortens the time to resolution of coronavirus disease (COVID-19) pneumonia and lowers the highest and last CT scores from sequential chest CT. *AJR Am J Roentgenol* 2020 Mar;30:1–7.